Original Article

High resolution imaging and quantification of the nailfold microvasculature using optical coherence tomography angiography (OCTA) and capillaroscopy: a preliminary study in healthy subjects

Li-Bin Dong[1], Ying-Zhao Wei[1], Gong-Pu Lan[2,3,4], Jia-Tao Chen[1], Jing-Jiang Xu[2,3,4], Jia Qin[2,3,4], Lin An[2,3,4], Hai-Shu Tan[2,3], Yan-Ping Huang[2,3,4]^

[1]School of Mechatronic Engineering and Automation, Foshan University, Foshan, China; [2]School of Physics and Optoelectronic Engineering, Foshan University, Foshan, China; [3]Guangdong-Hong Kong-Macao Joint Laboratory for Intelligent Micro-Nano Optoelectronic Technology, Foshan University, Foshan, China; [4]Innovation and Entrepreneurship Teams Project of Guangdong Pearl River Talents Program, Guangdong Weiren Meditech Co., Ltd., Foshan, China

Contributions: (I) Conception and design: YP Huang, LB Dong; (II) Administrative support: HS Tan, L An; (III) Provision of study materials or patients: GP Lan, JJ Xu, J Qin, L An; (IV) Collection and assembly of data: LB Dong, YZ Wei; (V) Data analysis and interpretation: LB Dong, GP Lan, JT Chen, JJ Xu, JQ, L An, HS Tan; (VI) Manuscript writing: All authors; (VII) Final approval of manuscript: All authors.

Correspondence to: Dr. Yan-Ping Huang. School of Physics and Optoelectronic Engineering, Foshan University, Foshan, Guangdong, China. Email: yale.huangyp@fosu.edu.cn.

Background: A wide range of diseases, such as systemic sclerosis, can be diagnosed by imaging the nailfold microcirculation, which is conventionally performed using capillaroscopy. This study applied optical coherence tomography angiography (OCTA) as a novel high resolution imaging method for the qualitative and quantitative assessment of the nailfold microvasculature, and compared OCTA imaging with capillaroscopy.

Methods: For qualitative assessment, high resolution OCTA imaging was used to achieve images that contained a wide field of view of the nailfold microvasculature through mosaic scanning. OCTA imaging was also used to observe the characteristic changes in the microvasculature under external compression of the upper arm. For quantitative evaluation, the capillary density and the capillary diameter of the nailfold microvasculature were assessed with both OCTA and capillaroscopy by repeated measurements over 2 days in 13 normal subjects. The results were analyzed using the intraclass correlation coefficient (ICC).

Results: OCTA imaging showed the typical nailfold microvasculature pattern, part of which was not directly seen with the capillaroscopy. OCTA imaging revealed significant changes in the nailfold microvasculature when a large external pressure was applied via arm compression, but no significant changes were observed using capillaroscopy. The capillary density measured by OCTA and capillaroscopy was 6.8±1.5 and 7.0±1.2 loops/mm, respectively, which was not significantly different (P=0.51). However, the capillary diameter measured by OCTA was significantly larger than that measured using capillaroscopy (19.1±2.5 *vs.* 13.3±2.3 μm, P<0.001). The capillary diameter measurements using OCTA and capillaroscopy were highly reproducible (ICC =0.926 and 0.973, respectively). While the capillary diameter measured with OCTA was significantly larger, it was rather consistent with the diameter measured using capillaroscopy (ICC =0.705).

Conclusions: This study demonstrated that OCTA is a potentially viable and reproducible tool for the imaging and quantification of the capillaries in the nailfold microvasculature. The results of this study provide a solid basis for future applications of OCTA in qualitative and quantitative assessment of nailfold microcirculation *in vivo*.

^ ORCID: 0000-0002-4430-3965.

Keywords: Nailfold microvasculature; optical coherence tomography angiography; capillaroscopy; quantification; reproducibility; intraclass correlation coefficient (ICC)

Submitted Jun 29, 2021. Accepted for publication Nov 11, 2021.
doi: 10.21037/qims-21-672
View this article at: https://dx.doi.org/10.21037/qims-21-672

Introduction

The skin is the outermost organ of the human body, providing thermal conservation, tactile sensation, and physical protection, all of which are largely maintained by the microcirculation. Indeed, the skin microcirculation can reflect both local and systematic health status, such as Raynaud's phenomenon (1), systemic sclerosis (2), and diabetes (3). Clinically, numerous approaches have been developed to investigate the changes in the microcirculation, including the vessel corrosion cast technique and medical imaging methods such as ultrasound, micro-computed tomography (CT) laser Doppler imaging, and capillaroscopy. However, these techniques have certain disadvantages when studying the skin microvasculature *in vivo*. For example, vessel casting is designed to be used for *in-vitro* or *in-situ* studies. Micro-CT imaging can be used for both *in vitro* and *ex vivo* investigations (4), but its associated disadvantages include the risk of ionizing radiation exposure, the need for contrast agent injection, and slow imaging speed for investigating the microcirculation. Ultrasound imaging is faster and suitable for real-time observations, but the spatial resolution of conventional clinical ultrasounds (3–6 MHz) is not sufficient for capillary imaging. Laser Doppler imaging (LDI) is capable of studying quantitative changes in the microcirculation in situations such as cold stimulus or acupuncture of the fingertips (5,6), however, it suffers from a lack of depth localization and adequate resolution for observing the changes in individual capillaries. Laser speckle imaging (LSI) can be used for tissue perfusion imaging (7). If specifically designed with a confined scan region and improved spatial resolution, LSI can be used to observe some capillaries (8), particularly the enlarged capillaries, however, it does not have sufficient depth resolution. Capillaroscopy is a convenient and inexpensive method with high spatial resolution that is used clinically for the direct observation of the microcirculation in some tissues, including the nailfold and oral mucosa (9). However, capillaroscopy is intrinsically a 2D imaging method with shallow penetration using visible light. Therefore, the development of technology that is fast and capable of providing 3D images of the microvasculature down to the microscale level of the individual capillary is urgently needed.

Optical coherence tomography-based angiography (OCTA) is a rapidly developing imaging modality that has attracted much attention for imaging the skin microcirculation *in vivo* (10-13). Recent OCTA technology is based on constructing the signal contrast of blood vessels using the more dynamic features of either phase, amplitude, or complex signal reflected from the vascular structure in repeated OCT scans (10,14). Different names for OCTA technologies have been coined in the literature, such as Doppler OCT (DOCT), dynamic OCT (dOCT), and optical microangiography (OMAG). All are used for the same purpose in general, but can be differentiated by their flow signal extraction algorithms (12). OCTA has distinct advantages, including non-invasiveness, depth-resolved 3D imaging, and fast acquisition speed, and therefore, it has been progressively applied to the study of skin-related diseases in dermatology and rheumatology.

An *et al.* [2010, 2011] pioneered the investigation of the microcirculation in skin tissue beds and demonstrated that the microvasculature was denser in skin with psoriasis than in normal skin (15,16). Subsequently, comprehensive studies have been conducted using OCTA to image the microvascular morphology of normal skin, and to assess vascular changes induced by inflammatory stimuli or skin lesions and wound healing (17-21). OCTA has been shown to produce highly repeatable measurements related to the skin microcirculation (22) and visualization of different vasculature patterns under OCTA has allowed the development of specific terminology related to the skin microcirculation (23). Therefore, broader clinical applications of OCTA in skin physiology and physiopathology are expected in the near future.

Many studies have investigated the use of OCTA in examining the skin microcirculation. However, they fail to assess the efficacy of OCTA against a comparative method. LDI has been used in some studies as a reference method,

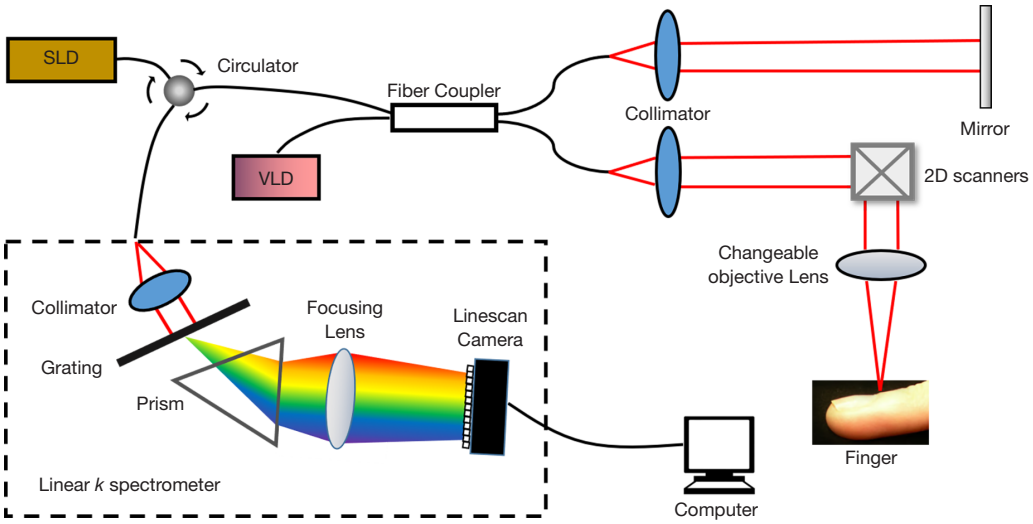

Figure 1 A schematic representation of the spectral domain optical coherence tomography (SD-OCT) system used for imaging the nailfold microvasculature. The changeable objective lens can be adjusted to alter the lateral resolution of the microvasculature image. SLD, superluminescent diode; VLD, visible laser diode.

but the comparison is indirect due to its inferior imaging resolution compared to OCTA (24). On the other hand, capillaroscopy can be used to directly observe the capillary network in the nailfold. Indeed, capillaroscopic examination of the nailfold microvasculature is a well-established clinical tool for the diagnosis of certain diseases, including systemic sclerosis and Raynaud's phenomenon (25). Capillaroscopy can also determine certain microvascular parameters, including capillary density and capillary size, which are important in identifying systemic sclerosis (26,27). Therefore, capillaroscopy may be a good reference standard for assessing the efficacy of OCTA.

Imaging the nailfold microvasculature with OCTA may have diagnostic significance for both local and systemic diseases. Numerous studies have used OCTA in qualitative imaging of the nailfold microvasculature morphology (28-31). For example, Baran *et al.* [2015] successfully adopted DOCT and ultra-high sensitive optical microangiography to observe the capillary flow and morphology within a human finger cuticle (29). Ring *et al.* [2016] used dynamic OCT to examine the typical functional and structural abnormalities of the nailfold microcirculation in a small number of patients with connective tissue diseases (30). Shahipasand *et al.* [2019] pioneered the imaging of nailfold capillaries using a commercial ophthalmic OCT instrument (31). However, detailed quantitative studies of the microvasculature parameters, such as the capillary diameter, using high resolution OCTA imaging and its validation against a reference method are still lacking.

This current study applied high resolution OCTA to the imaging and quantitative analysis of the nailfold microcirculation in a population of normal healthy subjects. Quantitative parameters, namely, the capillary density and capillary size, were extracted from the *en-face* OCTA images of the nailfold microvascular structure and directly compared with measurements obtained using capillaroscopy as a reference standard. The measurement reproducibility of these quantitative parameters was analyzed. We present the following article in accordance with the MDAR checklist (available at https://dx.doi.org/10.21037/qims-21-672).

Methods

Optical coherence tomography (OCT) and capillaroscopy imaging systems

A custom-built spectral domain OCT (SD-OCT) with a linear-k spectrometer was used in this study for imaging the nailfold microvasculature (32,33). A schematic of the SD-OCT system is shown in *Figure 1*. The system included a superluminescent diode light source (IPSDS1307C-1311, Inphenix Inc., Livermore, CA, USA) with a central wavelength of 1,290 nm and a –3 dB bandwidth of 80 nm (1,250–1,330 nm), a 50/50 fiber

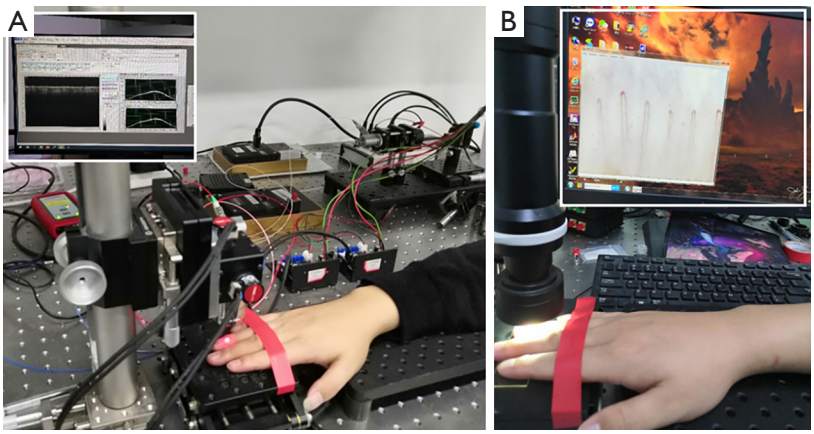

Figure 2 Imaging of the nailfold microvasculature at the fingertip using (A) the OCTA and (B) the capillaroscopy imaging systems. The sub-windows show the software interface of the two imaging systems in data acquisition. OCTA, optical coherence tomography angiography.

coupler, a linear-wavenumber spectrometer (PSLKS1300-001-GL, Pharostek, Rochester, MN, USA), and a high-speed linescan camera (GL2048L-10A-ENC-STD-210, Sensors Unlimited Inc., Princeton, NJ, USA) at an A-line acquisition rate of 76 kHz. The axial resolution was approximately 15.1 µm through experimental measurement of point spread function (22). To balance imaging range and lateral resolution, 2 different objective lenses with focal lengths 54 mm (Model LSM04, Thorlabs Inc. Newton, NJ, USA) and 18 mm (Model LSM02, the same brand) were used in the large and small fields of view imaging, with a lateral resolution of approximately 12.9 and 4.3 µm, respectively. Large field of view imaging was used to show the overall microcirculatory network, while the small field of view imaging was used to evaluate individual U-shaped capillaries. The control and data acquisition for OCTA imaging was accomplished using the Labview software (Version 2017, National Instruments, Austin, TX, USA). For OCTA microvasculature imaging, four repeated B-scans were used at each position to construct the vessel blood flow signal from the structural signal.

A commercial capillaroscope (Model BL-CG600, Belona Technologies Inc., Ezhou, Hubei, China) with a magnification power of ×400 was used to image the nailfold microvasculature. The capillaroscope connected via a USB cable to a computer where image sequences could be displayed in real time and saved for offline analysis. For nailfold microvasculature imaging, a series of 30 images was acquired in about one second, and the best image, as manually judged by the operator, was selected for the extraction of the microvascular parameters. The operation followed the general guidelines for the imaging of nailfold microcirculation using a capillaroscope (34), and cedarwood oil was used for tissue clearing prior to imaging. Video images (size 640×480) with a pixel resolution of 1.4 µm were acquired, which corresponds to a 2D field of 896 µm × 672 µm.

Experiments

A series of three experiments were conducted to demonstrate the feasibility of OCTA in nailfold microcirculation imaging. Specifically, imaging a wide field of view of the nailfold microvasculature, a repeatability study on the OCTA-derived quantitative measurements, and observation of the microvasculature changes under external pressure were performed. A typical setup for OCTA and capillaroscopy imaging is shown in *Figure 2*, where the fingertip is fixed underneath the imaging probe for imaging of the nailfold microvasculature.

This study was conducted in accordance with the Declaration of Helsinki (as revised in 2013) and was approved by the Research Ethics Committee of Foshan University (L2021130). Informed consent was obtained from all participants before experimentation.

Experiment 1: wide field OCTA nailfold microvasculature imaging

This experimental scan was conducted on the nailfold of the ring finger of a young male subject, aged 24 years (DLB). A montage scan protocol was designed to increase the field of view of the OCTA image through multiple zigzag scans using the 54 mm lens. A single scan grid included a field

of view of 3 mm × 3 mm, while the incremental step was 2 mm with an overlap of 1 mm. The 3D data acquisition time was approximately 10 seconds for the 3 mm × 3 mm scan with 400 A-lines collected in each B-mode image and 400 B-mode images in each volume, representing a scanning step of 7.5 μm in both directions. A total scan of 6×2 grids with an overall field of 13 mm × 5 mm was conducted for the wide field of view imaging.

Experiment 2: nailfold microvasculature imaging and reproducibility study

A direct comparison of OCTA imaging and capillaroscopy was conducted in 13 normal subjects, including 10 males and 3 females, with an average age of 21.6±2.8 years. None of the participants had any finger skin problems. The 18 mm lens was used to achieve better lateral resolution. The center part of the nailfold of the ring finger was used for imaging, as this area is relatively flat and enabled ease of focusing. The imaging area was 1 mm × 1 mm for the OCTA and 0.9 mm × 0.7 mm for capillaroscopy. The 3D data acquisition time was approximately 10 seconds for the 1 mm × 1 mm OCTA scan with 400 A-lines collected in each B-mode image and 400 B-mode images in each volume, representing a scanning step of 2.5 μm in both directions. A repeated measurement was performed by the same operator on the second day using the same protocols to assess the reproducibility of the two imaging methods. A black ink dot was marked at the edge of the nailfold to guide the alignment of the scan region of the two imaging methods. All experiments were conducted at 25 ℃, and the order of OCTA imaging and capillaroscopy was randomly selected. The data from this experiment are available upon request from the corresponding author of this paper.

Experiment 3: response of nailfold microcirculation to external pressure

In one subject (DLB), a pressure cuff applied to the upper arm was used to examine the response of the nailfold microcirculation to external pressure on the circulatory system. Prior to experimentation, the subject's blood pressure, including the systolic and the diastolic pressure, was measured. The nailfold microcirculation was measured under three states of external pressure, namely, no pressure, 40 mmHg, and middle blood pressure (the mean of the systolic and diastolic pressure). The OCTA and capillaroscopic imaging were conducted at half a minute after the external pressure was applied on the upper arm of the tested subject. The testing location was similar to that used in *Experiment 1*. Using OCTA imaging, regions of 3 mm × 3 mm and 1 mm × 1 mm were scanned with the 54 and 18 mm objective lens, respectively, under different upper arm compressions. The data acquisition time and the scanning steps used for each volume were identical to that in *Experiment 1* and *Experiment 2*. The subject was given a 30-minute rest period between two consecutive tests to allow for recovery.

Imaging processing and data analysis method

Optical coherence tomography angiography (OCTA) flow signal extraction and en-face image generation

The OCT structural signal was obtained using an inverse Fourier transform of the acquired spectral data based on the imaging principle of the spectral domain OCT. The OCTA flow signal was then extracted based on an eigendecomposition-based clutter filtering technique based on repeated B-scan data (35). The static structural signal and flow signal were separated from this processing, and the flow signals of each A-line in multiple B-scans were used to construct the volumetric OCTA data. A maximum intensity projection scheme was conducted in the approximate depth range of 0.135–4.790 mm to construct a 2D *en-face* image, which could then be directly compared to the capillaroscopy image acquired from the same region.

Extraction of quantitative microvascular parameters

Quantitative parameters related to the nailfold microvasculature, including the capillary density and the capillary diameter, were computed from the *en-face* OCTA and capillaroscopy images. Capillary density was calculated by counting the number of distal end capillary loops in a fixed distance along the microvasculature apex direction (loops/mm). The capillary diameter was calculated locally using an Otsu segmentation-based technique (36). Briefly, a small rectangular subregion, including the targeted capillary loop to be analyzed, was cropped from the raw image, and the adaptive thresholding segmentation method based on the Otsu's algorithm was used to segment the blood vessel. A morphological opening with a structuring element of 5×5 was used to remove isolated noisy pixels. An additional opening was conducted using a larger line structuring element if obvious horizontal strips were observed, which are a common artifact observed in OCTA imaging caused by subject motion (37). After vessel segmentation, a morphological thinning operation was used to obtain the vessel skeleton. Finally, the ratio between the area of the

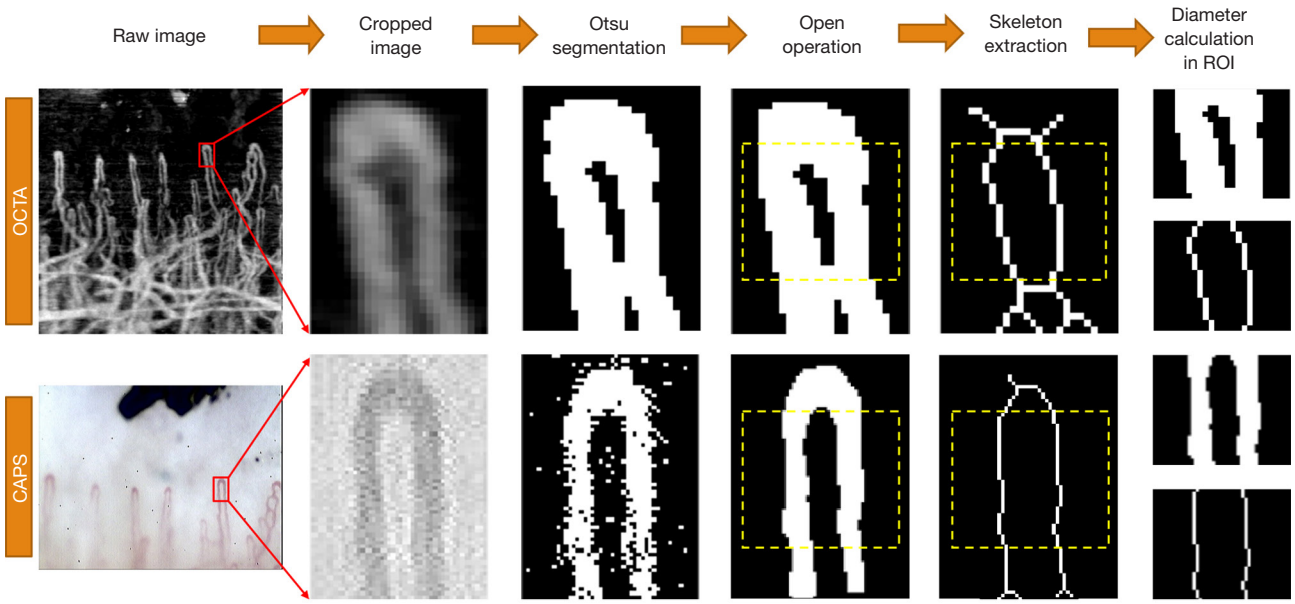

Figure 3 The processing steps involved in extracting the capillary diameter measurements from the OCTA image (the upper row) and the capillaroscopy image (the lower row), respectively. The main steps were image cropping, Otsu segmentation, morphological operation, skeleton extraction, and average diameter calculation in the selected region of interest (ROI). OCTA, optical coherence tomography angiography; CAPS, capillaroscopy.

segmented vessel and the length of its skeleton was used as the average capillary diameter. A region of 50 μm in length, which was approximately 25 μm beneath the loop apex, was selected as the region of interest for calculating the average capillary diameter. *Figure 3* shows the processing steps and the typical results obtained in the calculation of an average capillary diameter. For capillaroscopy images, the image processing step was conducted on a grayscale image converted from its raw color image. It should be noted that, due to heterogeneous image quality and distortion, not all capillaries could be used for an accurate measurement of the capillary diameter. Therefore, capillary-based rather than subject-based statistical analysis was used for the comparison of capillary diameter between two repeated measurements, and between OCTA and capillaroscopy. Candidate capillaries selected for the calculation of capillary diameter had no obvious distortion, no twisting, a peak intensity generally larger than 150/255 in grayscale, and good quality in all tests. The capillary diameter was extracted using custom-written Matlab (2017b, Mathworks, Natick, MA, USA) scripts based on the imaging processing toolbox.

Data analysis and statistics

In *Experiment 2*, the capillary diameter was calculated for several capillary loops in each subject. Each capillary loop was then counted as an individual sample for statistical analysis. A paired *t*-test was conducted to compare capillary diameter measurements from the two imaging methods. Furthermore, the intraclass correlation coefficient (ICC) was calculated, and Bland-Altman analysis was conducted to examine the reliability of the repeated measurements and the inter-method comparisons (between OCTA and capillaroscopy). The ICC [2,2], with measurement of absolute agreement, was used to estimate the reliability of the two repeated measures in OCTA and capillaroscopy imaging. The ICC [2,1], with measurement of consistency, was used to estimate the consistency of measurements between OCTA and capillaroscopy imaging (38). The ICC was categorized into the following four grades: poor (<0.40), fair (0.40–0.60), good (0.60–0.75), or excellent (≥0.75) (39). A P value <0.05 obtained using the SPSS software (IBM Inc., Chicago, IL, USA) was considered statistically significant.

Results

Experiment 1: *Figure 4* shows the results of a wide field of view of the nailfold microvasculature composed by

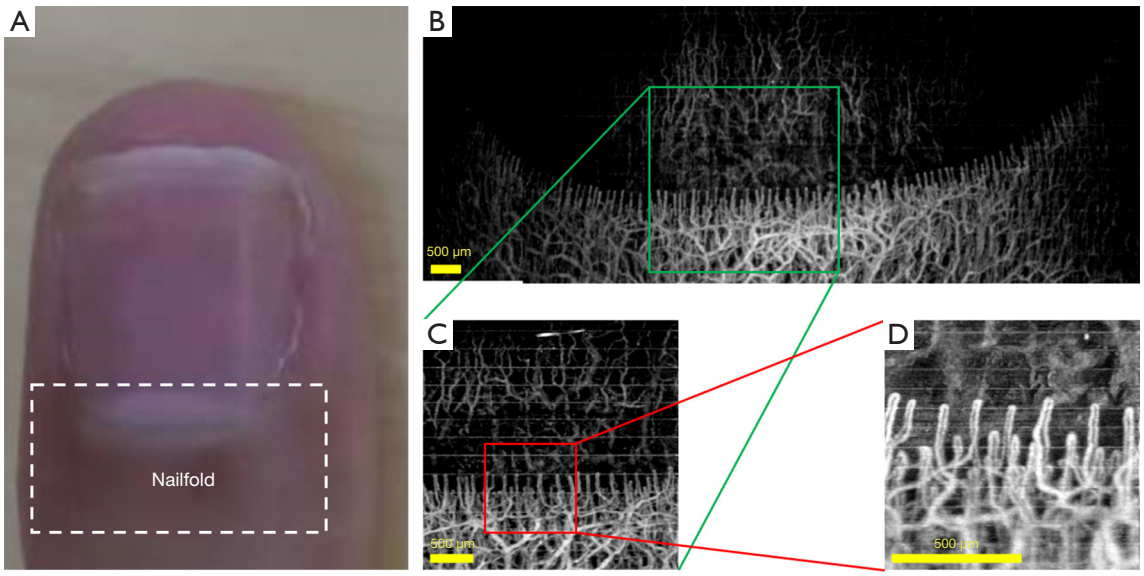

Figure 4 Wide and small fields of view of the nailfold microvasculature using OCTA imaging. (A) A photograph of the fingertip and the selected nailfold region for wide field OCTA imaging. (B) A wide field of view (13 mm × 5 mm) OCTA image of the nailfold microvasculature consisted of multiple small 3 mm × 3 mm scans (C) achieved using an objective lens with f=54 mm. (D) A small field of view (1 mm × 1 mm) OCTA image used for clear observation of capillary loops achieved using an objective lens with f=18 mm. The scale bars represent 500 μm in length. OCTA, optical coherence tomography angiography.

mosaicing multiple small field scans. The corresponding small field of view with a relatively high-resolution is shown, and the characteristic capillary loop (reversed U-shape) can be observed. A general comb-like structure of the microstructure can be clearly observed in the tip of the nailfold microvasculature (*Figure 4B*). At a certain distance proximal from the tip, the microvasculature becomes denser and more inter-connected, and discrimination of single vessels becomes more difficult. The quality of the image was better at the center compared to either side of the finger, which may be due to the curvature of the finger causing weaker signals when reflected from the sides. Some microvasculature was also observed in the tissue region under the nail. The reversed U-shape capillary loop could not be observed clearly using the 54 mm lens, but it could be clearly discriminated using the higher-resolution 18 mm lens (*Figure 4D*). Therefore, the quantitative analysis in *Experiment 2* was conducted using the data acquired from the 18 mm lens.

Experiment 2: typical images obtained using OCTA and capillaroscopy that were used for the calculation of capillary density and capillary diameter are shown in *Figure 5*. All capillaries visible with the capillaroscopy could also be observed with the OCTA. However, generally, more capillary loops could be observed in the OCTA images compared to the capillaroscopy images, which may be due to a larger depth of focus in OCTA compared to the capillaroscopy. No significant differences were detected between the first OCTA capillary density measurement (OCTA-1; 6.8±1.5 loops/mm) and the second measurement (OCTA-2; 6.9±1.6 loops/mm) (P=0.44; *Figure 6A*). The differences may have been caused by small discrepancies in the imaging region which may lead to inconsistencies in the number of capillary loops counted. Similarly, no significant differences were found between the first capillaroscopy capillary density measurement (CAPS-1; 6.9±1.1 loops/mm) and the second measurement (CAPS-2; 7.0±1.3 loops/mm) (P=0.34). As no significant differences were found between the two measurements for each method, the average of the first and second measurements was used to compare the capillary density between the two imaging methods. There was no significant difference in capillary density measurements between the 2 methods (OCTA: 6.8±1.5 *vs.* CAPS: 7.0±1.2 loops/mm; P=0.51).

A total of 52 pairs of capillary loops were selected for quantitative analysis and comparison between OCTA and capillaroscopy (*Figure 6B*). The results of the ICC and Bland-Altman analysis are tabulated in *Table 1* and

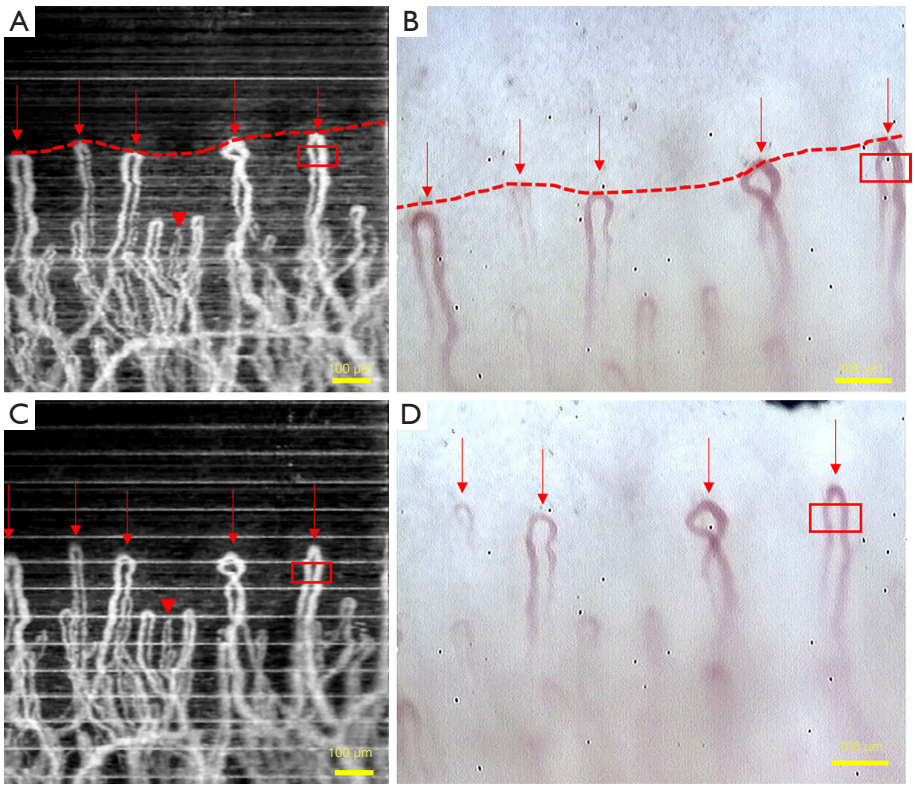

Figure 5 Repeated capillary density measurements in one finger were generated using OCTA (A,C) and capillaroscopy (B,D). The dotted lines show the end capillary apex direction used for counting capillaries in the density measurement. The red arrows show the capillaries selected for the calculation of capillary density along the apex direction. The arrowhead shows a capillary which was visible in OCTA but barely visible in capillaroscopy, although it was not counted in the capillary density measurement. The red rectangular window shows the region of interest (ROI) for the calculation of average capillary diameter. The scale bar indicates a length of 100 μm in each image. OCTA, optical coherence tomography angiography; CAPS, capillaroscopy.

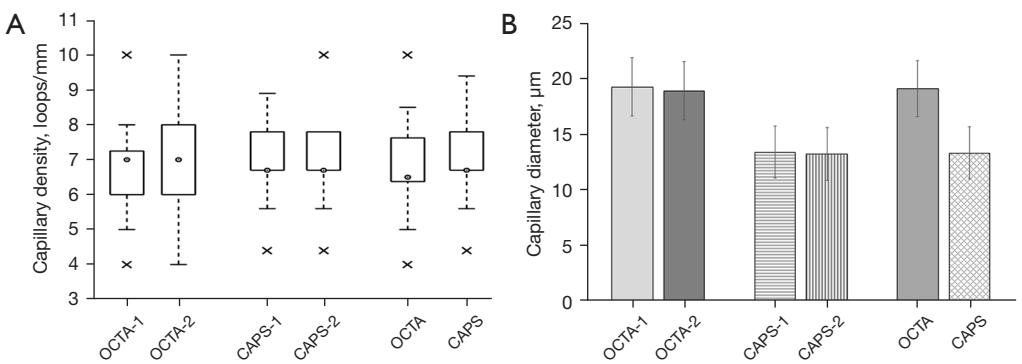

Figure 6 A comparison of the two repeated measurements using OCTA and capillaroscopy, and a comparison between OCTA and capillaroscopy. (A) A box plot of capillary density results, where the box represents the first and third quartile, the circle represents the median, and the cross represents the outliers. (B) A bar plot of capillary diameter, where the error-bars indicate standard deviation. OCTA, optical coherence tomography angiography.

Table 1 Capillary diameter measurements obtained using OCTA and capillaroscopy

Parameters	Mean Φ ± SD (μm)	ICC	95% CI of ICC	$\overline{d}$ (μm)	SD_d (μm)	95% LA (μm)
OCTA-1 *vs.* OCTA-2	19.3±2.6 *vs*. 18.9±2.6	0.926	0.870–0.958	–0.35	1.34	–2.98 to 2.28
CAPS-1 *vs.* CAPS-2	13.4±2.3 *vs*. 13.3±2.4	0.973	0.953–0.985	–0.13	0.76	–1.62 to 1.37
OCTA *vs.* CAPS	19.1±2.5 *vs*. 13.3±2.3***	0.705	0.537–0.820	–5.78	1.88	–9.46 to –2.11

OCTA, optical coherence tomography angiography; CAPS, capillaroscopy; OCTA-1; the first OCTA measurement; OCTA-2; the second OCTA measurement; CAPS-1, the first capillaroscopy measurement; CAPS-2, the second capillaroscopy measurement; ICC, intraclass correlation coefficient; CI, confidence interval; LA, limit of agreement; Φ, diameter; $\overline{d}$, the mean difference; SD_d, standard deviation of difference; ***, P<0.001.

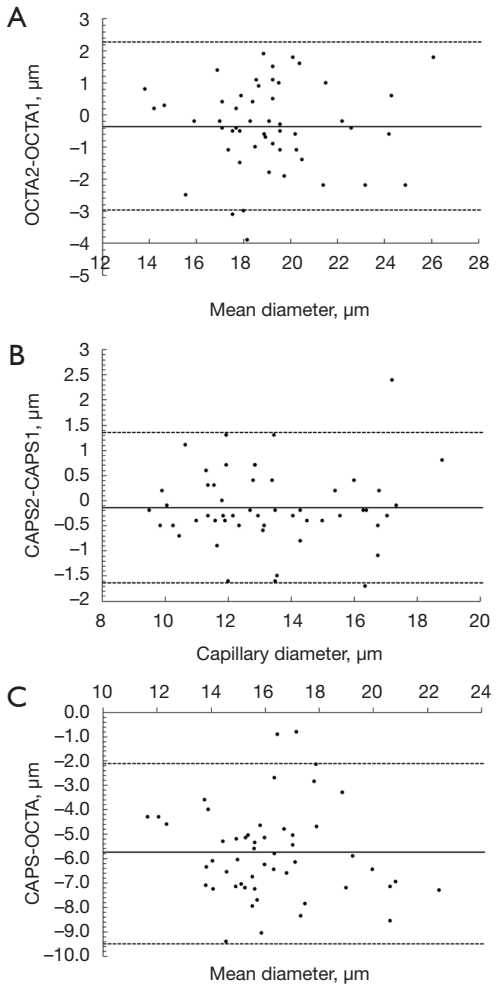

Figure 7 Bland-Altman plots showing the differences in capillary diameters between the two repeated measurements achieved using (A) OCTA and (B) capillaroscopy. (C) A Bland-Altman plot showing the difference in the averaged capillary diameter measured using OCTA imaging and capillaroscopy. The mean difference and the upper and lower 95% limit of agreement are shown as the solid line and the two dotted lines, respectively. OCTA, optical coherence tomography angiography.

Figure 7. There was no consistent difference in capillary size between the 2 repeated measurements using OCTA and the 2 repeated measurements using capillaroscopy (P>0.05). However, the capillary size measured using OCTA was significantly larger than that measured using capillaroscopy (P<0.001). The ICC between OCTA-1 and OCTA-2, and between CAPS-1 and CAPS-2 were 0.926 and 0.973, respectively. In terms of consistency, an ICC of 0.705 was found between the averaged OCTA and averaged capillaroscopy measurements of the capillary diameter, which suggested that the results of the two imaging methods were quite consistent.

Experiment 3: the changes in the nailfold microvasculature during the three-stage occlusion of the upper arm using an air puff was observed by OCTA imaging in a subject with a blood pressure of 95/65 mmHg. *Figure 8* shows the microvasculature of the nailfold under an external pressure of 0, 40 mmHg, and a middle blood pressure of 80 mmHg using the three different configurations. There was no obvious change in the microvasculature between 0 pressure and 40 mmHg external compression, that is, when the external pressure was lower than the diastolic pressure. However, when the external pressure was increased to the mean blood pressure, namely, 80 mmHg in this case, a significant weakening of the flow signal and discontinuity in the microvascular could be observed. This was more clearly observed in using the 54 mm lens. The OCTA image also displayed a periodic pattern of change in signal strength, which might be due to the periodic change in the blood flow speed in the microvascular vessels. Similarly, the capillaroscopy images showed no significant changes in the blood vessels upon application of external pressure up to 40 mmHg. However, when greater external pressure was applied (80 mmHg), the vessel pixel intensity increased and the vessel diameter looked thicker compared to its normal status under no pressure.

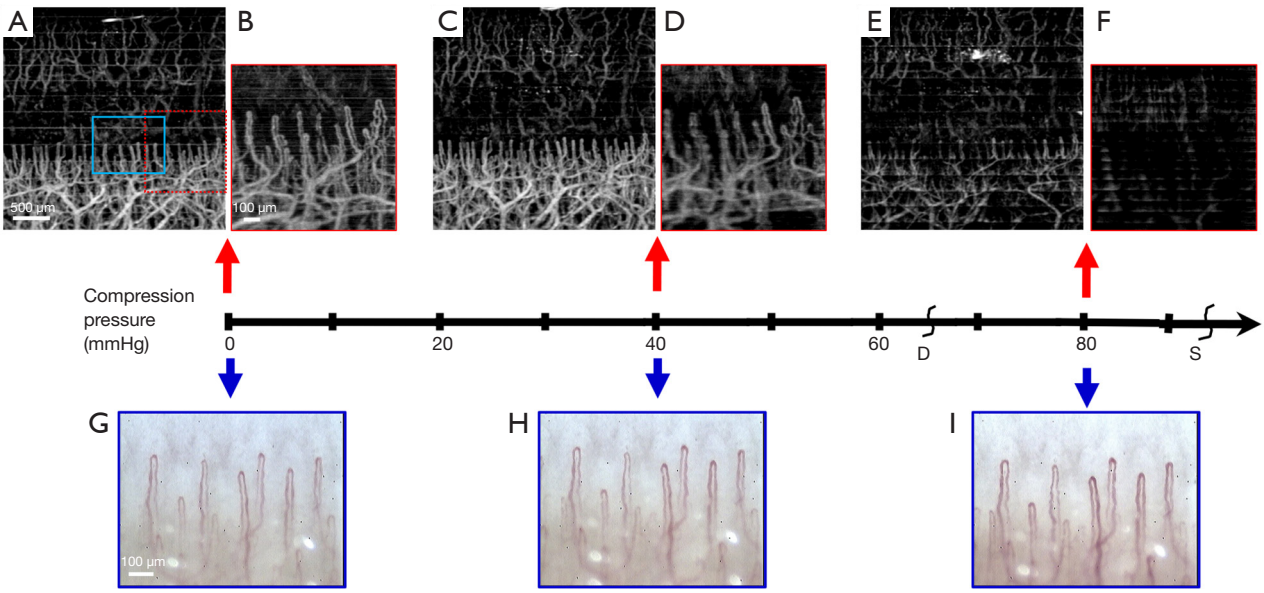

Figure 8 Microvasculature changes in response to increasing external occlusion pressures caused by compression of the upper arm. Microvasculature changes with (A) no external pressure, (C) 40 mmHg external pressure, and (E) 80 mmHg external pressure observed using OCTA imaging with the 54 mm objective lens. Microvasculature changes observed under (B) no external pressure, (D) 40 mmHg pressure, and (F) 80 mmHg pressure observed using OCTA imaging with the 18 mm objective lens. Microvasculature changes under (G) no external pressure, (H) 40 mmHg pressure, and (I) 80 mmHg pressure observed using capillaroscopy imaging. The blue rectangular window and the dotted red window in (A) show the approximate position where the capillaroscopy and the high resolution OCTA scan were conducted. The change in compression pressure and imaging time points are indicated by the horizontal axis. Scale bars of 100 μm or 500 μm are shown in each image. OCTA, optical coherence tomography angiography; S, the systolic pressure; D, the diastolic pressure.

Discussion

In this study, OCTA was used to image the nailfold capillaries and to provide a quantitative analysis of the capillary density and capillary size measurement. The quantitative analysis of repeated measurements showed that OCTA imaging of the nailfold capillaries was highly reproducible. OCTA also showed highly consistent measurements, but with a significantly larger vessel size compared to that achieved using capillaroscopic imaging. The key issues related to the methodology and results of this study are discussed as follows.

The three experiments were conducted to demonstrate the application of OCTA in studying nailfold microvasculature, including qualitative macroscopic larger field of view imaging, quantitative microvascular morphology analysis, and physiological applications.

Due to a large amount of data required in the volumetric scan and limited A-line acquisition speed, a small field of view, such as 3 mm × 3 mm, is generally used in OCTA imaging. This is sometimes insufficient for a full analysis of the whole nailfold microvasculature status. A wider field of view of the nailfold microvasculature can be achieved by mosaic scanning and consequent image registration or stitching, and this technique has been implemented in capillaroscopy imaging (40). The current study applied this technique to OCTA imaging. Imaging that has a wide field of view is very useful for specific applications, such as calculation of the average nailfold microvasculature density and disease screening for lesion localization. However, this technique can be hindered by a longer acquisition time, as well as the need to adjust the probe orientation at different scan positions due to the curvature of the finger. Further development of an artificial intelligence-controlled automatic scanning system or super-high speed OCT data acquisition system would facilitate wide field of view imaging and improve the practicality of this technology.

Capillary density and capillary size are important parameters in the diagnosis of potential diseases in patients. In this study, capillary density was calculated using a direct

observation method. Another popular method cited in the literature is the 90° method, which may produce slightly different results compared to the direct observational method (27). The difference between the various capillary counting methods in OCTA should be further evaluated in a clinical setting with a large subject population. In our study cohort, the mean capillary density obtained using the OCTA was 7 loops/mm in a population of 13 healthy subjects, and this was within the normal range of 6.1–11.0 loops/mm previously reported (27). No significant difference was found in the capillary density measurements using OCTA and capillaroscopy, suggesting that OCTA is also an effective method for assessing the capillary density of the nailbed. Considering the advantages of a larger depth of focus in infrared OCT imaging compared to visible light microscopy, some of the capillaries might be observed more clearly in OCTA than in capillaroscopy, therefore producing a larger capillary density. Further clinical studies should be conducted to identify whether factors such as aging, body location, gender, and ethnicity (34), affect capillary density.

Capillary size is also an important parameter in characterizing the changes in the microcirculation caused by disease. In this study, the capillary diameter measured using OCTA was 19 μm, and 13 μm using capillaroscopy. It should be noted the capillary diameter calculated in this study was an averaged value of the arterial limb and the venous limb in the selected processing region of interest of the capillary loop. The averaged capillary diameter measured by capillaroscopy was consistent with that reported in the literature (34,41). However, the measured value of the capillary diameter was significantly larger using OCTA compared to capillaroscopy ($P<0.001$). The difference in capillary size obtained from the two imaging modalities may be explained by the following reasons. First, the contrast mechanism is different for the two imaging modalities. OCTA is based on the change of infrared light reflection induced by blood flow in the capillary, while capillaroscopy is a microscopy technique using visible light reflection for direct observation of the capillary morphology. Therefore, the intensity distribution of the capillary in the two imaging modalities is different, which may affect the segmentation results and diameter calculations. Due to the laminar flow within blood vessels, the OCTA signal tends to be strongest in the center and weakest around the wall. This may result in a smaller diameter measurement using OCTA compared to capillaroscopy. Second, the lateral imaging resolution is different for the two imaging modalities. In our experiment, the lateral resolution of OCT (10 μm) in the focal region was inferior to that of capillaroscopy (<1 μm), which would increase the capillary diameter measurement results. Third, the difference in acquisition time may have caused distortion, and this might affect the measurement results. Compared to capillaroscopy, the acquisition time is longer in OCTA imaging, and thus, the distortion caused by finger motion in the data acquisition period may be greater. Considering that the fast axis is aligned with the cross section of the capillary, this effect of distortion caused by finger motion was considerably limited in the design of this study. Overall, the lateral resolution may result in a significantly larger capillary diameter measurement when using OCTA compared to capillaroscopy. Although the capillary diameter measured using OCTA was significantly larger than that measured with capillaroscopy, the results were consistent, as shown by a good ICC (0.705). This suggested that the capillary diameter measured using OCTA can be used as a quantitative parameter to reflect its physical dimension.

Reliability analysis based on two repeated measurements conducted over two days demonstrated that OCTA is a highly reproducible method for measuring capillary diameter even though the reliability coefficient ICC was slightly smaller in OCTA compared to capillaroscopy (0.926 *vs.* 0.973). A lower ICC in OCTA might be explained by the presence of more complicated and stricter acquisition conditions, which require proficient skills in the data collection process. These stringent conditions include the axial adjustment of the beam focus and the finger surface orientation to optimize signal quality. The judgement of optimal signal quality during the acquisition may also require more professional training and experience compared to that required to operate the capillaroscope. The signal quality was directly observed from a clear real-time image in capillaroscopy, while direct observation was not possible with OCTA. There is a paucity of literature evaluating the reproducibility of capillary diameter measurements using OCTA. However, recent studies have assessed the reproducibility of vessel density measurements using OCTA. Some investigations have reported similar ICC values for OCTA measurements of vessel density and indicated that signal quality is an important factor affecting measurement reproducibility (42). In our study, capillaries with relatively poor imaging quality were excluded from the diameter calculations to improve the measurement accuracy. This was based on the observation that the vessel quality obtained from OCTA imaging was not consistently

satisfactory. If these capillaries with poor quality had been included, the results of the quantitative analysis and comparison would be greatly affected. In our investigation, the OCTA measurement repeatability studies were conducted on healthy individuals. Previous studies using capillaroscopy have reported that patients with primary Raynaud's phenomenon have a capillary diameter 2-fold greater than that observed in healthy subjects, and patients with systemic sclerosis have a nailfold capillary diameter that is 3–4 times larger than that in control subjects (43). Giant capillaries, whose maximum widths can be 4–10 times larger than normal, are commonly observed in pathology (34). If the same measurement error is assumed and both patients and healthy subjects are included in the measurement repeatability study, the calculated ICC value would become greater due to the increased sample variation relative to the fixed measurement error. In general, this study demonstrated that both OCTA and capillaroscopy are highly reproducible methods for the quantitative measurement of the nailfold capillary diameter.

Experiment 3 demonstrated the dynamic changes in nailfold microvasculature under external compression of the upper arm. The appearance of the capillary network observed under the two imaging modalities was completely different. OCTA is a functional imaging technique that intrinsically indicates the flowability of the blood, therefore it is a direct reflection of the livingness of the capillary metabolism. In capillaroscopy, the capillary vitality can only be evaluated through multiple image sequences where the movement of red blood cells can be tracked and their velocity can be measured quantitatively (44). Under high external pressure compression of the upper arm, distortion of the microvasculature was more obvious under OCTA imaging. The discomfort experienced by the test subject may have affected finger control and motion, resulting in difficulty obtaining good image quality using the high resolution OCTA 18 mm lens (*Figure 8F*). Under low external pressure (40 mmHg), the high resolution OCTA image quality was degraded (*Figure 8D*), but degradation was less pronounced in the low resolution images obtained using the 54 mm lens (*Figure 8C*). Under substantial large external pressure, a periodic pattern of fluctuations in the capillary intensity along the slow scan axis was observed (*Figure 8E*), and this may be due to the periodic changes in the blood velocity in the capillary in a cardiac cycle. In the systolic stage, the blood flow in the capillary can be sensed by OCTA, however, in the diastolic phase, the blood velocity in the capillary can barely be sensed by OCTA, thereby causing a distinct bright and dark interweaving effect on the OCTA image. The capability of OCTA signal intensity to show meaningful physical metabolic blood flow activity suggests that it may be a potential research tool for examining microcirculation changes in certain tissue conditions such as pressure ulcers (45). It should be noted that there is some external pressure on the skin during the fixation of the fingertip for OCTA or capillaroscopy imaging. Choi *et al.* [2014] studied the effects of local external pressure on the microvascular perfusion in the nailfold region and revealed that changes in the pressure were closely correlated with capillary flow (46), suggesting that this effect should be carefully monitored during the imaging procedure. In our experiments, the fixation pressure was considered small, and this effect was controlled and therefore minimal.

In summary, this study demonstrated that OCTA is a potentially viable research tool for the imaging of the nailfold microvasculature when investigating the physiology of normal microcirculation and related diseases. Compared to capillaroscopy, OCTA is a 3D imaging method with a larger penetration depth, and thus has some advantages, such as resolving the capillary localization in the depth direction. This may be useful for counting and classifying the capillary loops when measuring the line density of the capillaries. However, capillaroscopy also has its own merits, such as the ability to provide quantitative blood flow velocity information if acquired with a high frame rate camera, which is currently not possible with OCTA (47). Clinically, capillaroscopy is much cheaper and has better spatial resolution than OCTA, and thus, it is unlikely to be replaced by OCTA in clinical applications in the near future.

There were some limitations to the current study. The study population was small and no clinical patients were involved in this investigation. Future studies involving larger populations of healthy participants, as well as patients with medical conditions, should be conducted to further validate these results. Algorithms for generating OCTA images and quantitative measurement techniques are developing rapidly. Advanced algorithms should be developed in the future to facilitate higher quality nailfold microvasculature images and to achieve more accurate diameter measurements (48-50). Furthermore, in addition to the capillary diameter, other quantitative parameters such as capillary width, loop width, and contrast of venous/arterial limbs (34), should be included in future studies to fully assess the potential of OCTA imaging in the morphological examination of the nailfold microvasculature.

Conclusions

In this study, the feasibility of using OCTA for imaging the nailfold microvasculature was assessed and compared with capillaroscopy as a reference method. The comb-like nailfold microvasculature could be observed clearly in the wide field of view OCTA images obtained with the 54 mm objective lens. However, quantitative capillary analysis was superior when higher lateral resolution imaging was performed with the 18 mm objective lens. Analysis of quantitative results, including the capillary density and the capillary diameter, showed that the OCTA measurements were highly reproducible. The capillary diameter measured using OCTA was significantly larger than that measured with capillaroscopy, but the results were consistent, as indicated by a good ICC. OCTA imaging demonstrated functional variations in the nailfold capillary flow under external compression of the upper arm. The changes in capillary flow were dependent on the compression pressure compared to the subject's blood pressure. OCTA is recommended as a viable tool in the basic research of nailfold microvasculature changes in circulation-related diseases, such as systemic sclerosis.

Acknowledgments

Funding: This study was partially supported by the National Natural Science Foundation of China (No. 61871130 to YPH), the Guangdong-Hong Kong-Macao Intelligent Micro-Nano Optoelectronic Technology Joint Laboratory (No. 2020B1212030010), and the Innovation and Entrepreneurship Teams Project of Guangdong Pearl River Talents Program (No. 2019ZT08Y105).

Footnote

Reporting Checklist: The authors have completed the MDAR checklist. Available at https://dx.doi.org/10.21037/qims-21-672

Conflicts of Interest: All authors have completed the ICMJE uniform disclosure form (available at https://dx.doi.org/10.21037/qims-21-672). Authors GPL, JJX, JQ, LA and YPH serve as consultants for the Guangdong Weiren Meditech Co., Ltd., whose products are ophthalmic devices. The other authors have no conflicts of interest to declare.

Ethical Statement: The authors are accountable for all aspects of the work in ensuring that questions related to the accuracy or integrity of any part of the work are appropriately investigated and resolved. The study was conducted in accordance with the Declaration of Helsinki (as revised in 2013). The study was approved by the Research Ethics Committee of the Foshan University (L2021130) and informed consent was obtained from all individual participants.

References

1. Mannarino E, Pasqualini L, Fedeli F, Scricciolo V, Innocente S. Nailfold capillaroscopy in the screening and diagnosis of Raynaud's phenomenon. Angiology 1994;45:37-42.
2. Cutolo M, Sulli A, Pizzorni C, Accardo S. Nailfold videocapillaroscopy assessment of microvascular damage in systemic sclerosis. J Rheumatol 2000;27:155-60.
3. Maldonado G, Guerrero R, Paredes C, Ríos C. Nailfold capillaroscopy in diabetes mellitus. Microvasc Res 2017;112:41-6.
4. Zagorchev L, Oses P, Zhuang ZW, Moodie K, Mulligan-Kehoe MJ, Simons M, Couffinhal T. Micro computed tomography for vascular exploration. J Angiogenes Res 2010;2:7.
5. Correa MJ, Andrade LE, Kayser C. Comparison of laser Doppler imaging, fingertip lacticemy test, and nailfold capillaroscopy for assessment of digital microcirculation in systemic sclerosis. Arthritis Res Ther 2010;12:R157.
6. Litscher G, Wang L, Huber E, Nilsson G. Changed skin blood perfusion in the fingertip following acupuncture needle introduction as evaluated by laser Doppler perfusion imaging. Lasers Med Sci 2002;17:19-25.
7. Heeman W, Steenbergen W, van Dam G, Boerma EC. Clinical applications of laser speckle contrast imaging: a review. J Biomed Opt 2019;24:1-11.
8. Liu R, Qin J, Wang RK. Motion-contrast laser speckle imaging of microcirculation within tissue beds in vivo. J

Biomed Opt 2013;18:060508.
9. Chojnowski MM, Felis-Giemza A, Olesińska M. Capillaroscopy - a role in modern rheumatology. Reumatologia 2016;54:67-72.
10. Kashani AH, Chen CL, Gahm JK, Zheng F, Richter GM, Rosenfeld PJ, Shi Y, Wang RK. Optical coherence tomography angiography: A comprehensive review of current methods and clinical applications. Prog Retin Eye Res 2017;60:66-100.
11. Gao SS, Jia Y, Zhang M, Su JP, Liu G, Hwang TS, Bailey ST, Huang D. Optical Coherence Tomography Angiography. Invest Ophthalmol Vis Sci 2016;57:OCT27-36.
12. Deegan AJ, Wang RK. Microvascular imaging of the skin. Phys Med Biol 2019;64:07TR01.
13. Liu M, Drexler W. Optical coherence tomography angiography and photoacoustic imaging in dermatology. Photochem Photobiol Sci 2019;18:945-62.
14. Huang Y, Zhang Q, Thorell MR, An L, Durbin MK, Laron M, Sharma U, Gregori G, Rosenfeld PJ, Wang RK. Swept-source OCT angiography of the retinal vasculature using intensity differentiation-based optical microangiography algorithms. Ophthalmic Surg Lasers Imaging Retina 2014;45:382-9.
15. An L, Qin J, Wang RK. Ultrahigh sensitive optical microangiography for in vivo imaging of microcirculations within human skin tissue beds. Opt Express 2010;18:8220-8.
16. Qin J, Jiang J, An L, Gareau D, Wang RK. In vivo volumetric imaging of microcirculation within human skin under psoriatic conditions using optical microangiography. Lasers Surg Med 2011;43:122-9.
17. Lindsø Andersen P, Olsen J, Friis KBE, Themstrup L, Grandahl K, Mortensen OS, Jemec GBE. Vascular morphology in normal skin studied with dynamic optical coherence tomography. Exp Dermatol 2018;27:966-72.
18. Schuh S, Holmes J, Ulrich M, Themstrup L, Jemec GBE, De Carvalho N, Pellacani G, Welzel J. Imaging Blood Vessel Morphology in Skin: Dynamic Optical Coherence Tomography as a Novel Potential Diagnostic Tool in Dermatology. Dermatol Ther (Heidelb) 2017;7:187-202.
19. Manfredini M, Liberati S, Ciardo S, Bonzano L, Guanti M, Chester J, Kaleci S, Pellacani G. Microscopic and functional changes observed with dynamic optical coherence tomography for severe refractory atopic dermatitis treated with dupilumab. Skin Res Technol 2020;26:779-87.
20. Deegan AJ, Wang W, Men S, Li Y, Song S, Xu J, Wang RK. Optical coherence tomography angiography monitors human cutaneous wound healing over time. Quant Imaging Med Surg 2018;8:135-50.
21. Deegan AJ, Mandell SP, Wang RK. Optical coherence tomography correlates multiple measures of tissue damage following acute burn injury. Quant Imaging Med Surg 2019;9:731-41.
22. Men SJ, Chen CL, Wei W, Lai TY, Song SZ, Wang RK. Repeatability of vessel density measurement in human skin by OCT-based microangiography. Skin Res Technol 2017;23:607-12.
23. Ulrich M, Themstrup L, de Carvalho N, Ciardo S, Holmes J, Whitehead R, Welzel J, Jemec GBE, Pellacani G. Dynamic optical coherence tomography of skin blood vessels - proposed terminology and practical guidelines. J Eur Acad Dermatol Venereol 2018;32:152-5.
24. Zugaj D, Chenet A, Petit L, Vaglio J, Pascual T, Piketty C, Bourdes V. A novel image processing workflow for the in vivo quantification of skin microvasculature using dynamic optical coherence tomography. Skin Res Technol 2018;24:396-406.
25. Smith V, Herrick AL, Ingegnoli F, Damjanov N, De Angelis R, Denton CP,, et al. Standardisation of nailfold capillaroscopy for the assessment of patients with Raynaud's phenomenon and systemic sclerosis. Autoimmun Rev 2020;19:102458.
26. van den Hoogen F, Khanna D, Fransen J, Johnson SR, Baron M, Tyndall A,, et al. 2013 classification criteria for systemic sclerosis: an American college of rheumatology/ European league against rheumatism collaborative initiative. Ann Rheum Dis 2013;72:1747-55.
27. Emrani Z, Karbalaie A, Fatemi A, Etehadtavakol M, Erlandsson BE. Capillary density: An important parameter in nailfold capillaroscopy. Microvasc Res 2017;109:7-18.
28. Subhash HM, Leahy MJ. Microcirculation imaging based on full-range high-speed spectral domain correlation mapping optical coherence tomography. J Biomed Opt 2014;19:21103.
29. Baran U, Shi L, Wang RK. Capillary blood flow imaging within human finger cuticle using optical microangiography. J Biophotonics 2015;8:46-51.
30. Ring HC, Themstrup L, Banzhaf CA, Jemec GB, Mogensen M. Dynamic Optical Coherence Tomography Capillaroscopy: A New Imaging Tool in Autoimmune Connective Tissue Disease. JAMA Dermatol 2016.
31. Shahipasand S, Mohammed-Noriega J, Sim D, Gizzi C, Kortum K. Nailfold capillaroscopy with a commercially available optical coherence tomography angiography for

ophthalmic use. Adv Ophthalmol Vis Syst 2019;9:38-42.
32. Lan G, Xu J, Hu Z, Huang Y, Wei Y, Yuan X, Liu H, Qin J, Wang Y, Shi Q, Zeng J, Shi Y, Feng J, Tan H, An L, Wei X. Design of 1300 nm spectral domain optical coherence tomography angiography system for iris microvascular imaging. J Phys D Appl Phys 2021;54:264002.
33. Hu Z, Rollins AM. Fourier domain optical coherence tomography with a linear-in-wavenumber spectrometer. Opt Lett 2007;32:3525-7.
34. Etehad Tavakol M, Fatemi A, Karbalaie A, Emrani Z, Erlandsson BE. Nailfold Capillaroscopy in Rheumatic Diseases: Which Parameters Should Be Evaluated? Biomed Res Int 2015;2015:974530.
35. Yousefi S, Zhi Z, Wang RK. Eigendecomposition-based clutter filtering technique for optical micro-angiography. IEEE Trans Biomed Eng 2011.
36. Otsu N. A threshold selection method from gray-level histograms. IEEE Trans Syst Man Cybern Syst 1979;9:62-66.
37. Spaide RF, Fujimoto JG, Waheed NK. Image artifacts in optical coherence tomography angiography. Retina 2015;35:2163-80.
38. McGraw KO, Wong SP. Forming inferences about some intraclass correlation coefficients. Psychol Methods 1996;1:30-46.
39. Cicchetti D. Guidelines, criteria, and rules of thumb for evaluating normed and standardized assessment instrument in psychology. Psychol Assess 1994;6:284-90.
40. Anderson ME, Allen PD, Moore T, Hillier V, Taylor CJ, Herrick AL. Computerized nailfold video capillaroscopy--a new tool for assessment of Raynaud's phenomenon. J Rheumatol 2005;32:841-8.
41. Bhushan M, Moore T, Herrick AL, Griffiths CE. Nailfold video capillaroscopy in psoriasis. Br J Dermatol 2000;142:1171-6.
42. Lee TH, Lim HB, Nam KY, Kim K, Kim JY. Factors Affecting Repeatability of Assessment of the Retinal Microvasculature Using Optical Coherence Tomography Angiography in Healthy Subjects. Sci Rep 2019;9:16291.
43. Bukhari M, Herrick AL, Moore T, Manning J, Jayson MI. Increased nailfold capillary dimensions in primary Raynaud's phenomenon and systemic sclerosis. Br J Rheumatol 1996;35:1127-31.
44. Wu CC, Lin WC, Zhang G, Chang CW, Liu RS, Lin KP, Huang TC. Accuracy evaluation of RBC velocity measurement in nail-fold capillaries. Microvasc Res 2011;81:252-60.
45. Mervis JS, Phillips TJ. Pressure ulcers: Pathophysiology, epidemiology, risk factors, and presentation. J Am Acad Dermatol 2019;81:881-90.
46. Choi WJ, Wang H, Wang RK. Optical coherence tomography microangiography for monitoring the response of vascular perfusion to external pressure on human skin tissue. J Biomed Opt 2014;19:056003.
47. Zhu J, Merkle CW, Bernucci MT, Chong SP, Srinivasan VJ. Can OCT Angiography Be Made a Quantitative Blood Measurement Tool? Appl Sci (Basel) 2017;7:687.
48. Wei W, Cogliati A, Canavesi C. Model-based optical coherence tomography angiography enables motion-insensitive vascular imaging. Biomed Opt Express 2021;12:2149-70.
49. Cheng Y, Chu Z, Wang RK. Robust three-dimensional registration on optical coherence tomography angiography for speckle reduction and visualization. Quant Imaging Med Surg 2021;11:879-94.
50. McDowell KP, Berthiaume AA, Tieu T, Hartmann DA, Shih AY. VasoMetrics: unbiased spatiotemporal analysis of microvascular diameter in multi-photon imaging applications. Quant Imaging Med Surg 2021;11:969-82.

Cite this article as: Dong LB, Wei YZ, Lan GP, Chen JT, Xu JJ, Qin J, An L, Tan HS, Huang YP. High resolution imaging and quantification of the nailfold microvasculature using optical coherence tomography angiography (OCTA) and capillaroscopy: a preliminary study in healthy subjects. Quant Imaging Med Surg 2022;12(3):1844-1858. doi: 10.21037/qims-21-672

